Experimental characterization of the monotonic and cyclic behaviour of a new dry-horizontal joint between precast walls

Aléxia Brandão[1], Sajjad Hosseini[2], André Furtado[3], Ricardo Carmo[4], Romain Sousa[5], Yllnor Tmava[6], Wanchai Detphan[7], Wit Derkowski[8] and Eduardo Júlio[9]

[1]CERIS – Instituto Superior Técnico, Portugal, alexia.ribeiro@tecnico.ulisboa.pt

[2]CERIS – Instituto Superior Técnico, Portugal, seyedsajjad.hosseini@tecnico.ulisboa.pt

[3]CERIS – Instituto Superior Técnico, Portugal, andre.furtado@tecnico.ulisboa.pt

[4]CERIS – Instituto Superior de Engenharia de Coimbra, Portugal, carmo@isec.pt

[5]Vigobloco SA, CERIS – Universidade de Aveiro, Portugal, romains@vigobloco.pt

[6]Linnaeus University, Sweden, yt222dh@student.lnu.se

[7]Linnaeus University, Sweden, wd222bi@student.lnu.se

[8]Linnaeus University, Sweden, wit.derkowski@lnu.se

[9]CERIS – Instituto Superior Técnico, Portugal, eduardo.julio@tecnico.ulisboa.pt

Abstract

The seismic behaviour of precast concrete modular constructions depends highly on the connections between structural elements, particularly those located in the horizontal joints in wall-based structural systems. Several dry and wet connection solutions have been developed in recent years, but most of them require complex assembly processes and additional concrete casting or were not designed to be seismic-resistant. Also, the possibility of having easy access to connection replacement in the case of seismic damage needs to be considered. The paper presents the design conception, detailing and testing of four types of a dry connection for horizontal joints between insulated bearing walls. The behaviour of the connection is investigated through a testing campaign of full-scale specimens subjected to tensile axial monotonic tests and tensile cyclic loading tests. The results are discussed in terms of force-displacement curves, tensile capacities and failure modes. The results showed a promising strength and deformation capacity when adequate detailing near the connection is ensured.

1 Introduction

The sustainability of building structures is becoming an increasingly important concern, gaining recognition alongside structural safety. Traditional cast *in-situ* concrete structures and prefabricated concrete structures with wet-type connections typically require long construction times due to extensive on-site activities [1]. Moreover, these structures behave as monolithic systems, meaning that when significant damage occurs or they reach the end of their lifespan, demolition is often necessary based on current construction technologies or very extensive repairing/retrofitting interventions. Consequently, this cycle leads to high energy consumption and significant environmental impacts, making it a major concern for sustainable construction [2]. To address these challenges, structures designed with deconstruction or reuse concepts have been investigated in recent years [3, 4].

Given the recent uncertainties caused by climate change, where extreme events are becoming increasingly frequent, along with crises such as war, future construction must adopt the design for deconstruction and reconstruction concept. With this objective in mind, the precast concrete wall panel system with bolted connections emerges as an effective solution to these evolving challenges. Load-bearing wall systems are commonly used in residential buildings due to their architectural flexibility, ease of manufacturing, and strong structural performance [5]. These systems involve the on-site assembly of prefabricated wall panels—which can be single, double, or feature integrated acoustic/thermal insulation—combined with hollow-core or double-T slab systems. Their high structural efficiency, particularly in moderate to high seismic regions, stems from their superior lateral force resistance compared to frame structures. However, there remains a notable gap in the literature regarding the seismic performance of these structural systems with dry connections. In this approach, bolted joints are specifically engineered to withstand tensile forces, shear forces, or both. Research indicates that steel tension bolts are widely used in beam-column connections [2, 6]; however, their application in structures primarily composed of load-bearing walls is far less common. Additionally, a detailed analysis of the load-bearing wall in the region surrounding the bolted connection has not yet been conducted. For instance, the study by Zhao, et al. [7] focused solely on the global lateral behavior of load-bearing walls with bolted connections, without performing experimental investigations on the detailing of the connection zone.

As part of the R2U Technologies – Modular Systems research project, a novel structural system is being developed, consisting of insulated load-bearing walls connected through bolted connections, in line with the design for deconstruction and reconstruction concept, as illustrated in Figure 1. Both vertical and horizontal joints utilize the same type of connection; however, they are subjected to different loading demands. The primary advantage of using insulated load-bearing walls is their reduced weight, which has a significant impact on transportation efficiency and contributes to a lighter overall building structure, thereby enhancing seismic performance. At the same time, these walls offer superior thermal insulation, reducing the need for additional insulation layers in compliance with current energy regulations. This connection system is designed to minimize the use of steel materials and heavy steel connectors (e.g., wall shoes or steel profiles) while allowing for rapid assembly and easy repair or disassembly in the case of an accidental load, eg. an earthquake. To ensure a safe and reliable seismic response, a detailed investigation of the connections between load-bearing walls is crucial, with particular emphasis on those forming the horizontal joints.

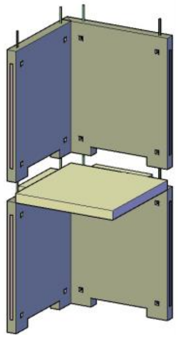

Fig. 1 Load-bearing wall resisting system with dry connections for residential buildings: a) 3D schematic layout.

The response of four types of bolted horizontal joints were experimentally tested under axial tensile force or single-character cyclic loading. The design concept and detailing of the four connection types will be thoroughly presented and compared. Then, their tensile capacity will be evaluated, through a testing campaign involving full-scale specimens subjected to monotonic and cyclic tensile loading, in terms of force-displacement curves and failure modes.

2 Testing campaign

The proposed structural system consists of insulated load-bearing walls with a total thickness of 22 cm, subdivided into three sections. The top and bottom ends of the wall are solid concrete, while the middle section comprises two 80 mm thick concrete layers separated by a 60 mm thick EPS (expand-

ed polystyrene) thermal insulation layer. The solid zones at the top and bottom of the wall were designed to absorb the forces transmitted through the wall connections. The connections between walls are made using bolts that pass through a preformed hole in the middle of the wall thickness, extending to a small square opening (10×10 cm²). A steel plate at the edge of the opening is to distribute the stress applied by the bolt, ensuring better load transfer and connection efficiency. Each wall is expected to have potentially 4 openings, allowing it to be used for both vertical and horizontal connections between walls, as shown in Figure 2. This paper focuses only on the connections for horizontal joints.
An experimental program was carried out involving a total of seven connection typologies for horizontal joints, aimed at studying the effects of i) the extension of the solid concrete at the top end of the wall, ii) the arrangement of reinforcing reinforcement bars (horizontal and vertical) around the opening where the steel bolt is positioned; and iii) the cyclic loading.
To conduct this study, a simplified approach was adopted by analyzing a single connection, enabling a more comprehensive characterization of the effects of the studied variables, as illustrated in Figure 2a. For this purpose, a representative wall specimen (see Figure 2a) with only one connection was constructed, and a common geometry was maintained across all groups (Figure 2b). To streamline the analysis, this paper presents results from groups 2, 3, 4, and 6, whose key variables are detailed in Figure 3. Each group consists of three specimens, allowing for the evaluation of experimental variability as well as the impact of cyclic loading. The geometry and reinforcement detailing are presented in subsection 2.1.

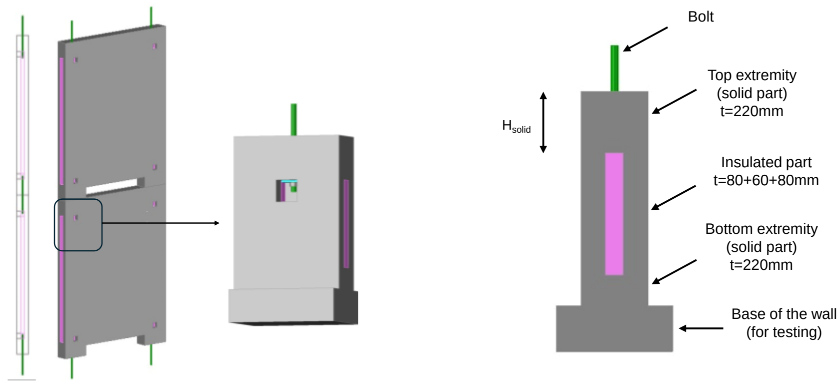

Fig. 2 Load-bearing walls with bolted connections: (a) Representative single-connection specimen of the proposed structural system; (b) Profile view of the single connection specimen, highlighting common characteristics.

2.1 Geometry and reinforcement detailing

Each specimen has a total height of 0.50 m, a width of 0.70 m, and a thickness of 0.22 m. Additionally, each specimen includes a foundation part with a thickness of 0.40 m, designed to secure the wall in place during testing. All walls were reinforced with a ϕ5/200 mm mesh near both faces of the wall. The main variations between the four groups are: i) Different lengths of the solid concrete zone at the top extremity (100 mm or 200 mm); and ii) Variations in the relative positioning of the vertical and horizontal reinforcement bars (type 1 and type 2 reinforcing rebars, respectively).

In the Group 2 specimens (Figure 3a), a 200 mm solid concrete zone was adopted at the top extremity. Type 1 and Type 2 reinforcing rebars were positioned away from the opening (Configuration 1). Although Group 2 specimens share the same solid concrete extension as Group 3, the arrangement of Type 1 and Type 2 reinforcing rebars differs. In Group 2, a 132 mm spacing was adopted between Type 1 rebars, allowing one pair of vertical rebars to be positioned close to the opening, while the other pair was placed further away (Configuration 2). The same Configuration 2 was also applied to Type 2 rebars.

In Group 4 (Figure 3c), a shorter solid concrete zone of 100 mm was adopted, and Configuration 1 was used for both Type 1 and Type 2 reinforcing rebars. Finally, in Group 6 (Figure 3d), a 100 mm solid concrete zone was also adopted; however, Type 1 and Type 2 reinforcing rebars followed a Configuration 2 layout. A detailed illustration of the Type 1 and Type 2 reinforcement configurations is presented in Figure 3e.

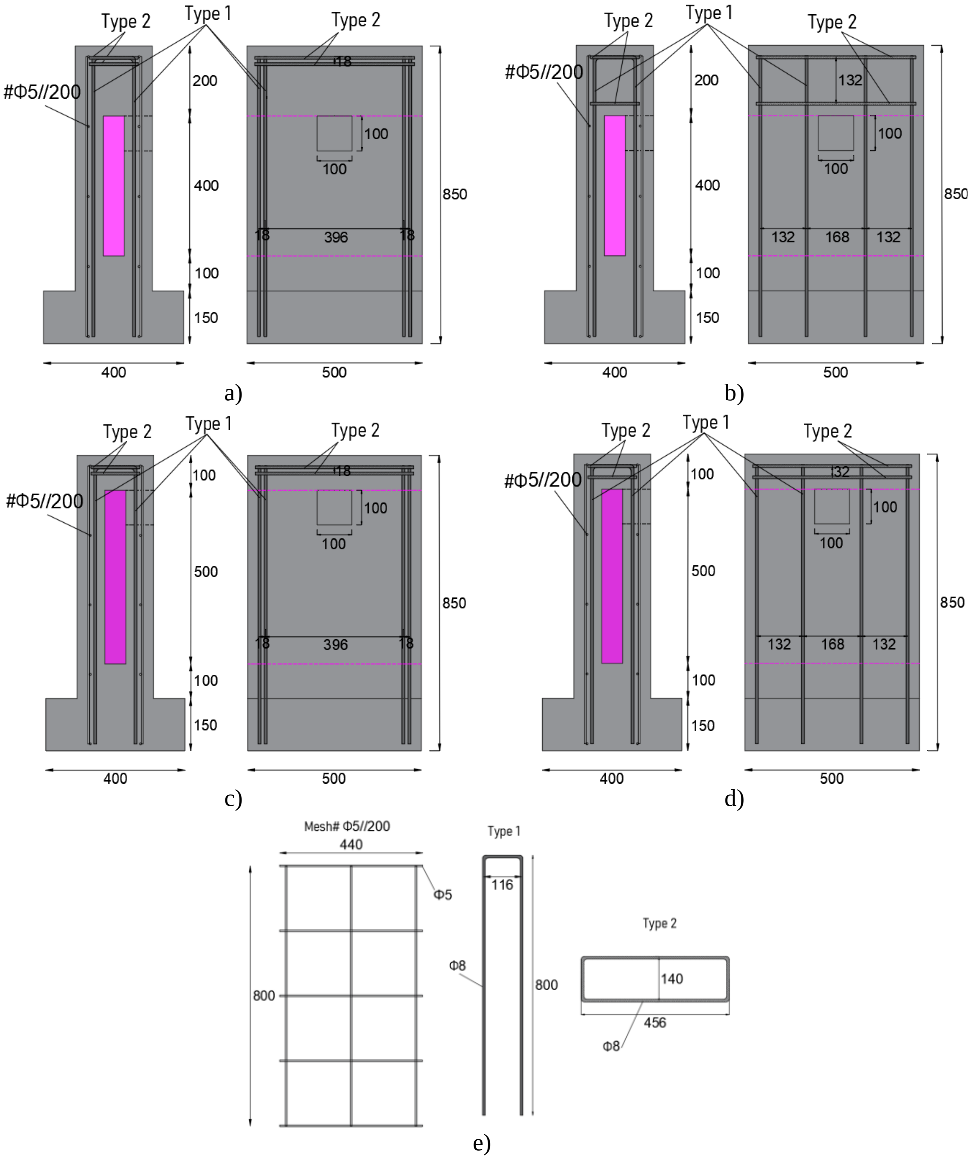

Fig. 3 Geometry and reinforcement detailing of the specimens: a) Group 2, b) Group 3, c) Group 4, d) Group 6, and e) mesh and type 1 and 2 rebars configuration.

2.2 Material properties

The materials used in this study include C50/60 class concrete, A500 NR reinforcements, and 8.8-grade threaded rebars (for the bolt). For C50/60 concrete, as specified in Eurocode 2 [8], the characteristic compressive strength is 50 MPa, the tensile strength is 4.1 MPa, and the elastic modulus is 35 GPa. In the experimental tests from three concrete cubes, the concrete exhibited a mean compressive strength of 68 MPa at 28 days. The characteristic strength can be estimated as f_{cm} minus 1.64×standard deviation [8]. Given a standard deviation of 2.15 MPa, the experimental characteristic strength is approximately 64.5 MPa, indicating higher than specified material strength and low dispersion. The steel used for concrete reinforcement was A500 NR, with a theoretical yield strength of 500 MPa and an elastic modulus of 200 GPa. Additionally, tensile tests were conducted on 8.8-grade threaded steel rebars with an internal diameter of 20.5 mm. The obtained stress-strain curve indicated an average yield strength of approximately 808 MPa, corresponding to the end of the linear segment, and an average maximum stress of approximately 1000 MPa (CoV: 1%).

2.3 Test setup, instrumentation, and loading protocol

Each - test was conducted using an Instron 5989 Series testing machine, where the base of each wall was fixed using steel profiles with a fastening mechanism, as shown in Figure 4, preventing vertical displacement of the walls' support. The four steel U-shape profiles were fixed to the Instron by bolts. The upper 2 (one each side) were fixed to the bottom 4 profiles (in this connection the holes are ovalized) to allow for some adaptation of the assembly inaccuracies. The load was applied directly to the connection bolt via a hydraulic servo-actuator, which was fixed to the Instron.
Displacements were measured using five LVDTs positioned as follows: two vertical LVDTs at the top of the wall (one on each side, LVDT 1 and LVDT 2), two LVDTs at the bottom of the specimen (LVDT 4 and LVDT 5), and one LVDT positioned at the mid-height level on the backside of the wall (LVDT 4). The data was recorded at a sampling frequency of 1 Hz.
The tests were conducted 28 days after specimen casting, following a standardized testing protocol. The first test in each group was a monotonic tensile strength test performed under displacement control at a rate of 0.01 mm/s (samples tested this way were marked with the letter M at the end of the symbol). From the resulting force-displacement curve, the yield displacement (d_y) was estimated, which was then used to define the loading protocol for the subsequent cyclic test. The second test in each group was a cyclic tensile test, also performed under displacement control at 0.01 mm/s (samples marked with the letter C at the end of the symbol). The cyclic loading protocol consisted of three cycles at each of the following target displacements: 0.25 d_y, 0.50 d_y, 0.75 d_y, d_y, 2d_y, 3d_y, etc., until specimen failure was observed. Finally, the third test in each group was another monotonic tensile test, conducted under the same displacement control rate of 0.01 mm/s as the first test.

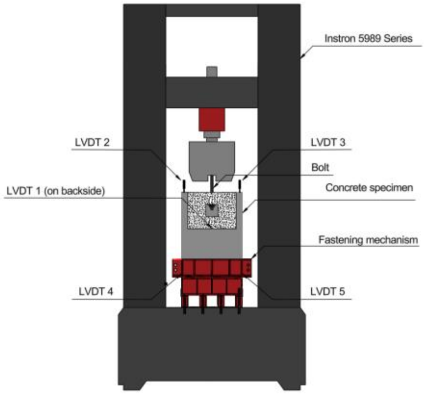

a)

b)

Fig. 4 Testing campaign: a) Schematic layout of the test setup; b) General view of the experimental setup.

3 Discussion of results

3.1 Tests results by group

The results analysis is conducted through the evaluation of force-displacement curves, where key points corresponding to yielding, peak force, and conventional failure are identified. The yield displacement (δy) and yield force (Fy) were determined following the methodology outlined in Annex B of Eurocode 8 [24], which defines an idealized force-displacement relationship to establish the yielding point of the curve. Conventional failure was considered as a 20% strength reduction after the peak load. Additionally, the initial stiffness was calculated between 30% and 60% of the maximum load for each specimen. Finally, the failure modes were analyzed and compared across different groups.

3.1.1 Group 2

The force-displacement curves of the three specimens from Group 2, shown in Figure 5a, exhibit a highly consistent response across all specimens under both monotonic and cyclic loading conditions, which allowed the conclusion that the type of loading did not affect the performance. The initial stiffness of specimen G2_3_M reached 45 kN/mm, which is approximately 17% higher than G2_2_C and 22% higher than G2_1_M. Regarding the peak load, the results were remarkably similar among the three specimens, with no significant influence of cyclic loading on this parameter. The highest peak load was recorded by G2_3_M at 188 kN, which is 17% higher than G2_2_C and 4.7% higher than G2_1_M. This indicates that both monotonically loaded specimens achieved comparable maximum strengths, while the cyclically loaded specimen exhibited a slightly lower peak strength. The displacement at peak load was similar for all three specimens, with differences of less than 17%. However, some variability was observed in the displacement at conventional failure, where G2_1_M reached the highest displacement (11.7 mm), approximately 26% greater than G2_3_M, which recorded the lowest displacement. Overall, the average peak strength among the specimens was 176 kN, with a low CoV of 8%, demonstrating consistent structural performance across the tested specimens.

Regarding the observed failure mode, an asymmetrical cracking pattern was identified on both faces of the specimens due to the presence of the opening. On the front face (where the opening is located), two main crack patterns were observed: a horizontal crack aligned with the top of the opening, extending across the entire width of the wall, and a vertical crack that propagated from the top of the opening to the top of the wall (see Figure 5b). On the back face, inclined cracks were observed originating from the central region, corresponding to the alignment where the opening in the wall ends, as shown in Figure 5c. The cracking pattern was more distributed on this face, indicating the ability to redistribute tensile stresses within the solid concrete zone.

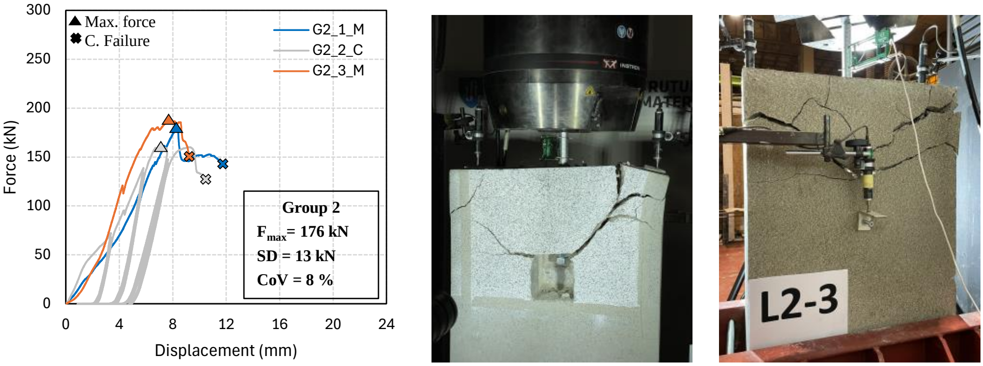

a) b) c)

Fig. 5 Group 2 results: a) force-displacement curves; b) failure mode - front view; and c) failure mode - back view.

3.1.2 Group 3

The Group 3 specimens exhibited a very similar performance in terms of force-displacement curves (see Figure 6a). The initial stiffness of specimens G3_3_M and G3_2_C was nearly identical, both reaching 18 kN/mm. Regarding peak load, the specimens subjected to monotonic loading, G3_1_M and G3_3_M, achieved comparable maximum forces of approximately 226 kN and 216 kN, respectively. In contrast, cyclic loading appeared to have an effect on reducing the ultimate strength of specimen G3_2_C, which reached 199 kN, approximately 12% and 8% lower than G3_1_M and G3_3_M, respectively. In terms of displacement at peak load, G3_2_C reached its maximum force first at 11.6 mm displacement, followed by G3_1_M and G3_3_M, which exhibited 11% and 19% higher displacements, respectively. Finally, conventional failure occurred at very similar displacement levels, with differences of less than 6% between specimens. Overall, the Group 3 specimens exhibited an average peak strength of 214 kN, with a coefficient of variation (CoV) of 6%, which can be considered low.

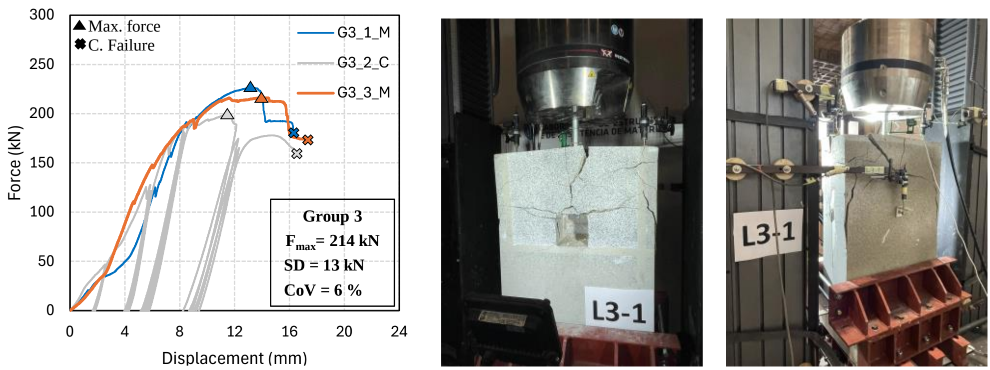

a) b) c)

Fig. 6 Group 3 results: a) force-displacement curves; b) failure mode - front view; and c) failure mode - back view.

Regarding the observed failure modes, all specimens displayed a similar failure pattern, characterized by widespread cracking on the front face, as shown in Figure 6b. However, a primary horizontal crack was observed, aligned with the top of the opening, as well as a second vertical crack extending from the center of the opening. On the back face, generalized cracking was also observed, with a pronounced 45º crack propagating from the top edge of the opening toward the contact point at the upper extremity of the wall, as illustrated in Figure 6c.

3.1.3 Group 4

The performance of the Group 4 specimens was characterized by very low strength capacity and limited deformation ability, as evident in the force-displacement curves presented in Figure 7a. The initial stiffness of specimen G4_2_C (20.86 kN/mm) was approximately 55% and 85% higher than that of G4_1_M and G4_3_M, respectively. Contrary to the trends observed in the previous groups, the cyclically loaded specimen (G4_2_C) reached the highest peak strength, approximately 91.6 kN, followed by G4_3_M and G4_1_M, with 21% and 45% lower strengths, respectively. Additionally, the maximum strength was reached at lower displacement values in G4_2_C (3.5 mm), whereas G4_1_M and G4_3_M exhibited 9% and 51% higher displacements, respectively. Finally, conventional failure occurred at similar deformation levels in the monotonically loaded specimens (approximately 6 mm), while G4_2_C failed at a 50% lower deformation level, likely due to the effect of the cyclic loading. Overall, the average strength for Group 4 was 75 kN, with a CoV of 22%.

The failure mode was characterized by a brittle failure mechanism, marked by cover concrete spalling at the top of the specimens and a combination of a horizontal main crack (aligned with the top of the opening) and a vertical one in the middle of the opening towards the top extremity was reported, as shown in Figure 7b. In addition, a symmetrical trapezoidal cracking pattern on the back face, as illustrated in Figure 7c. All specimens exhibited limited cracking in the concrete above the opening, which can likely be attributed to the shorter length of the solid concrete zone. This reduced the effectiveness of tensile force transmission to the vertical reinforcement bars, preventing the reinforcement from fully engaging and limiting crack propagation within the concrete.

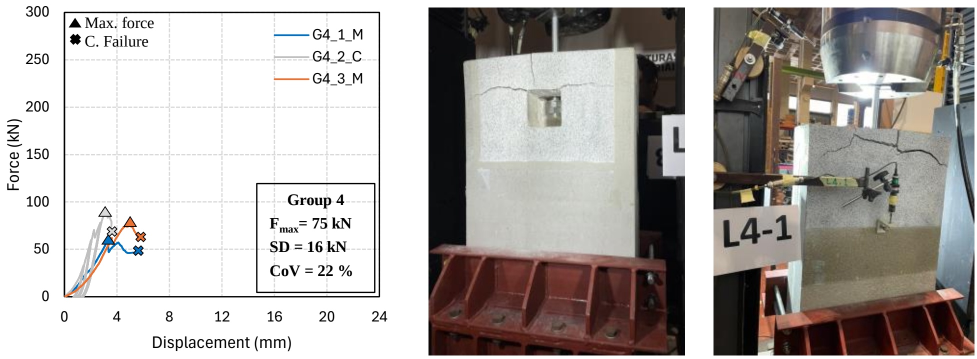

a) b) c)

Fig. 7 Group 4 results: a) force-displacement curves; b) failure mode - front view; and c) failure mode - back view.

3.1.4 Group 6

The performance of the Group 6 specimens was characterized by greater variation in behaviour among all specimens across all response parameters. The highest initial stiffness was observed in specimen G6_1_M, reaching 31.2 kN/mm, followed by G6_3_M and G6_2_C, which were approximately 38% and 59% lower, respectively. Regarding peak strength, the highest value was recorded in G6_1_M, with 100.6 kN, followed by G6_3_M and G6_2_C, which exhibited 22% and 32% lower strengths, respectively. Similarly, the maximum load capacity was reached at lower displacement values in G6_1_M (4.6 mm), followed by G6_3_M and G6_2_C, which had 23% and 46% higher displacements, respectively. This suggests that cyclic loading may have contributed to a reduction in peak load capacity and led to higher displacement values at peak load. Finally, conventional failure occurred first in specimen G6_3_M, at a displacement of 6.2 mm, while the other two specimens reached conventional failure at a displacement level 21% higher. Overall, Group 6 exhibited an average peak strength of 90 kN, with a CoV of 17%.

The failure mode exhibited different behavior on the front and back surfaces of the specimens. On the front face, an inclined cracking pattern was observed, originating from the upper corners of the opening and propagating toward both the lateral edge and the upper extremity, as illustrated in Figure 8b. On the back face, the cracking pattern was more dispersed, with two primary cracks visible: one horizontal crack aligned with the top of the opening, and another located near the upper edge of the wall, corresponding to cover concrete spalling, as shown in Figure 8c.

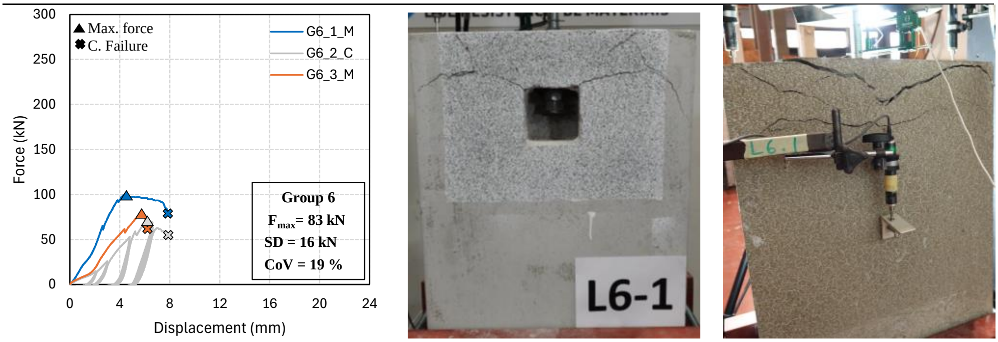

a) b) c)

Fig. 8 Group 6 results: a) force-displacement curves; b) failure mode - front view; and c) failure mode - back view.

3.2 Comparative analysis of the results

A global comparative analysis was conducted across the four groups, focusing on the average values of peak strength, the corresponding displacement at peak load, and the displacement at conventional failure. Regarding peak strength (Figure 9a), it was observed that Groups 2 and 3, which had 20 cm of solid concrete at the top extremity, reached higher strength values compared to Groups 4 and 6, which had only 10 cm of solid concrete. This clearly indicates that increasing the solid concrete zone improves the transfer of tensile forces to the vertical reinforcement bars, enabling the formation of a 45º tensile stress cone. Additionally, the presence of reinforcement bars (both vertical and horizontal) near the opening contributed to an increase in the connection's load capacity. This effect was observed in both 20 cm and 10 cm solid concrete groups, although the increase in strength was less pronounced for the 10 cm groups. Overall, Group 3 exhibited the highest average strength of 214 kN, followed by Groups 2, 6, and 4, with peak strength values of 18%, 62%, and 65% lower, respectively. It was also noted that a larger solid concrete zone above the opening resulted in a lower CoV (coefficient of variation). This may be attributed to the more brittle failure behavior observed in Groups 4 and 6, where concrete cover spalling at the top of the wall led to fragile failure mechanisms.

Regarding the displacement at peak strength (Figure 9b), similar trends were observed, which can be explained by the previously mentioned factors. The larger solid concrete zone contributed to higher deformation capacity before reaching peak load. Additionally, the presence of reinforcement bars near the opening further increased the displacement at peak strength. Group 3 reached peak strength at an average displacement of 12.9 mm, which was 1.66, 2.31, and 3.46 times higher than in Groups 2, 6, and 4, respectively. Finally, conventional failure followed the same patterns observed earlier. Group 3 reached conventional failure at an average displacement of 16.8 mm, approximately 1.60, 2.29, and 3.39 times greater than Groups 2, 6, and 4, respectively.

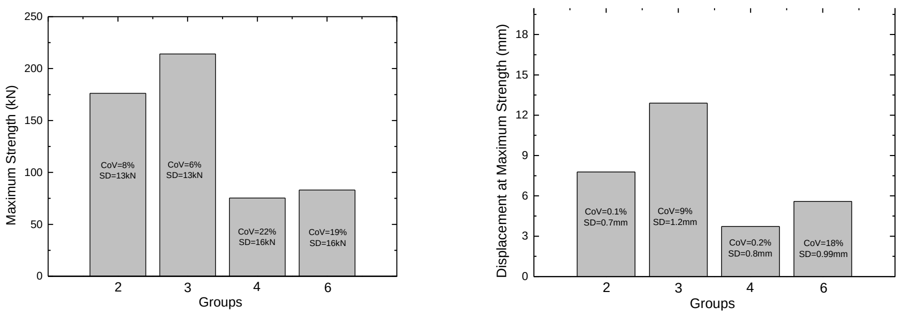

a) b)

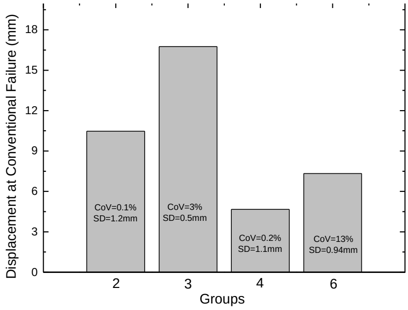

c)

Fig. 9 Global comparison: a) maximum strength; b) displacement at maximum strength; and c) displacement at conventional failure.

4 Final remarks

This study investigated the seismic performance of bolted connections in insulated load-bearing walls, designed in alignment with the design for deconstruction and reconstruction concept. An experimental program was conducted on four connection configurations, assessing their tensile capacity under monotonic and cyclic loading conditions.

The results highlight that the extension of the solid concrete zone at the top extremity of the wall and the reinforcement bar arrangement significantly influence the structural performance of the connections. The peak strength varied among groups, with Group 3 exhibiting the highest average strength (214 kN), followed by Groups 2, 6, and 4, which were 18%, 62%, and 65% lower, respectively. The presence of reinforcement bars near the opening contributed to an increase in load-bearing capacity, and this effect was more pronounced in the 20 cm solid concrete groups compared to the 10 cm groups.

Regarding deformation capacity, Group 3 achieved peak strength at an average displacement of 12.9 mm, which was 1.66, 2.31, and 3.46 times higher than in Groups 2, 6, and 4, respectively. Conventional failure displacement followed the same trend, with Group 3 reaching failure at 16.8 mm, 1.60, 2.29, and 3.39 times higher than Groups 2, 6, and 4, respectively. The CoV was lowest in Groups 2 and 3, indicating more consistent performance, whereas Groups 4 and 6 exhibited a higher CoV, likely due to brittle failure mechanisms associated with concrete cover spalling.

From a failure mode perspective, a horizontal crack aligned with the top of the opening, along with a vertical crack extending toward the upper wall extremity, was consistently observed. Specimens with shorter solid concrete zones (Groups 4 and 6) exhibited more brittle failures, characterized by cover concrete spalling and less effective stress transfer to the vertical reinforcement bars.

These findings reinforce the importance of optimizing the solid concrete zone and reinforcement placement in bolted wall connections to enhance seismic resilience and structural efficiency. Future research should focus on full-scale cyclic tests under realistic seismic conditions, integrating additional optimized reinforcement detailing to further improve structural performance and damage control in modular precast systems.

Acknowledgments

The authors acknowledge the support of Fundação para a Ciência e Tecnologia (FCT) which finances the authors' research centre, CERIS—Civil Engineering Research and Innovation for Sustainability with the funding reference UIDB/04625/2020. This article is a result of the Innovation Pact "R2UTechnologies|modular systems" (C644876810-00000019) by "R2UTechnologies" Consortium, co-financed by NextGeneration EU, through the Incentive System "Agendas para a Inovação Empresarial" ("Agendas for Business Innovation"), within the Recovery and Resilience Plan (PRR).

References

[1] F. Simões, F.-J. Rios-Davila, H. Paiva, H. Maljaee, M. Morais, and V. M. Ferreira, "Sustainability Evaluation Using a Life Cycle and Circular Economy Approach in Precast Concrete with Waste Incorporation," *Applied Sciences*, vol. 11, no. 24, p. 11617, 2021. [Online]. Available: https://www.mdpi.com/2076-3417/11/24/11617.

[2] R. Martins, R. d. Carmo, H. Costa, and E. Júlio, "A review on precast structural concrete walls and connections," *Advances in Structural Engineering*, vol. 26, no. 14, pp. 2600-2620, 2023, doi: 10.1177/13694332231191073.

[3] G. Resta and S. Gonçalves, "Design for disassembly and cultural sites. The use of modular architecture and prefabrication in exhibition venues," *Vitruvio*, Article vol. 9, no. 1, pp. 124-141, 2024, doi: 10.4995/vitruvio-ijats.2024.21442.

[4] J. He, S. Feng, G. Vasdravellis, and T. Liu, "Cyclic inelastic performance evaluation of locking bolt demountable shear connectors in steel-concrete composite structures," *Engineering Structures*, vol. 318, p. 118690, 2024/11/01/ 2024, doi: https://doi.org/10.1016/j.engstruct.2024.118690.

[5] fib, "Bulletin 74: Planning and design handbook on precast building structures," 2014.

[6] B. Zhao, D. Wu, and H. Zhu, "New modular precast composite shear wall structural system and experimental study on its seismic performance," *Engineering Structures*, vol. 264, p. 114381, 2022/08/01/ 2022, doi: https://doi.org/10.1016/j.engstruct.2022.114381.

[7] F. Zhao, F. Xiong, G. Cai, H. Yan, Y. Liu, and A. Si Larbi, "Performance and numerical modelling of full-scale demountable bolted PC wall panels subjected to cyclic loading," *Journal of Building Engineering*, vol. 63, p. 105556, 2023/01/01/ 2023, doi: https://doi.org/10.1016/j.jobe.2022.105556.

[8] IPQ, "EN 1992-1-1:2004 Eurocode 2: Design of concrete structures - Part 1-1: General rules and rules for buildings," 2004.